Available online at www.sciencedirect.com

SciVerse ScienceDirect

Ceramics International 39 (2013) 4801–4811

CERAMICS INTERNATIONAL

www.elsevier.com/locate/ceramint

Influence of Bi^{3+} as a sensitizer and SiO_2 shell coating as a protecting layer towards the enhancement of red emission in $LnVO_4$: Bi^{3+}, Eu^{3+} @ SiO_2 (Ln=Gd, Y and Gd/Y) powder phosphors for optical display devices

U. Rambabu[a,*], N.R. Munirathnam[a], S. Chatterjee[b], B. Sudhakar Reddy[c], Sang-Do Han[d]

[a]*Centre for Materials for Electronics Technology (C-MET), IDA Phase-III, Cherlapally, Hyderabad, India*
[b]*Department of Electronics and Information Technology (DeitY), Lodi Road, New Delhi, India*
[c]*S.V. Degree College, Department of Physics, Kadapa, India*
[d]*Korea Institute of Energy Research (KIER), Daejeon 305-343, Republic of Korea*

Received 12 November 2012; received in revised form 16 November 2012; accepted 23 November 2012
Available online 2 December 2012

Abstract

Enhanced red luminescence in $LnVO_4$: Bi^{3+}, Eu^{3+} @ SiO_2 phosphors has been improved mainly in three stages by investigating the effects of: (i) host composition (Gd, Y and Gd/Y), (ii) co-doping Bi^{3+} as a sensitizer and finally (iii) SiO_2 shell coating. XRD data revealed that the produced phosphors possess crystalline, pure phase with tetragonal structure. Silica coating on phosphor particles have been characterized by SEM/EDAX, TEM, PL and with the presence Si–O–Si, Si–O vibrational modes from the FT-IR spectra. Absorption band edges due to VO_4^{3-}, shifted to higher wavelength with Bi-concentration, owing to the presence of Bi–O bond in addition to V–O. The emission intensities of $^5D_0 \rightarrow {}^7F_2$ transition are stronger than $^5D_0 \rightarrow {}^7F_1$; indicating the lower inversion symmetry near Eu^{3+}, ions. Red emission intensity due to the efficient energy transfer from VO_4^{3-} to Eu^{3+} via Bi^{3+} ions in $Y_{0.949}VO_4$: $Bi^{3+}_{0.001}$, $Eu^{3+}_{0.05}$ phosphor was improved significantly, i.e. 1.6 times compared to $Y_{0.95}VO_4$: $Eu^{3+}_{0.05}$. This was further enhanced 2.25 times by SiO_2 shell coating. Thus, $Y_{0.949}VO_4$: $Bi^{3+}_{0.001}$, $Eu^{3+}_{0.05}$ @ SiO_2 are suggested to be a promising red phosphor for application in display devices or lighting.

Keywords: A. Powder: Chemical preparation; C. Color; C. Optical properties

1. Introduction

The research on rare-earths (RE) doped luminescent materials is always the most active field owing to the large need in the illumination and display field. For example in fluorescent lamps (FL), cathode ray tubes (CRTs), field emission displays (FEDs), plasma display panels (PDPs) and the newly emerging white light emitting diodes (WLEDs) [1–5]. Moreover, the active research is in progress for the efficient down-conversion and up-conversion phosphors to improve the power conversion efficiency of c-silicon solar cells, based on spectral conversion phenomena [6,7]. Most of the luminescent materials are oxides, sulfides and oxysulfides doped with transition metals or rare earth ions [8–10]. As for as the hosts concern, rare earth vanadates, especially yttrium vanadate (YVO_4) has been shown to be among the best candidates possessing high luminescence efficiency [11,12]. YVO_4: Eu^{3+} is known as a typical commercial red emitting phosphor used in lighting and cathode ray tubes [1]. In particular YVO_4: Eu^{3+} is strongly an attractive material as a red emitting phosphor in PDPs because of its high red color purity [13], which is caused by a non-centro symmetric site of Eu^{3+} ion [5]. Eu^{3+} ions occupy Y^{3+} site in YVO_4 lattices, resulting in hypersensitive transitions in the emission spectra [14]. YVO_4 crystallizes in the tetragonal zircon ($ZrSiO_4$) type structure

*Corresponding author. Tel.: +91 40 27267309.
E-mail addresses: urlagaddalar@gmail.com, rambabu32@rediffmail.com (U. Rambabu).

0272-8842/$ - see front matter © 2012 Elsevier Ltd and Techna Group S.r.l. All rights reserved.
http://dx.doi.org/10.1016/j.ceramint.2012.11.070

[15]. The vanadate is well excited by ultraviolet (UV) light and the photoluminescence quantum yield of the Eu^{3+} emission reaches as high as 70% [13]. In addition, $GdVO_4$: Eu^{3+} is a good red emitting material for displays because it absorbs UV light well, transfers energy efficiently from the host lattice (VO_4^{3-}) to the activator Eu^{3+}, ions. The PL intensity of $GdVO_4$: Eu^{3+} is of the same order as that of YVO_4: Eu^{3+} [5]. To achieve highly efficient emission from the lanthanide (Ln^{3+}) ions, host sensitization via energy transfer from the excited host to the Ln^{3+} ions is one of the effective ways. This might overcome the low absorption of the parity forbidden Ln^{3+}, 4f–4f transitions. Bi^{3+} ions with $6S^2$ electronic configuration can function both as an activator and a sensitizer for luminescent materials [7,16,17]. Bi^{3+}, ions not only enhances the luminescent intensity but also broadens the excitation spectra [18–20]. It has been demonstrated that the luminescence of Eu^{3+}, Sm^{3+} or Er^{3+} can be greatly enhanced through the resonant energy transfer from Bi^{3+} to Eu^{3+}, Sm^{3+} or Er^{3+}, ions [21,22]. YVO_4: Bi^{3+}, Eu^{3+} upon the excitation of near-UV light emits red through the charge transfer (CT) transition from Bi^{3+} to V^{5+} 3d, followed by the energy transfer to Eu^{3+} [23]. It is well known that the grain size, morphology, agglomeration or surface passivation can have a great influence on the PL properties of the phosphors [24–26]. Silica (SiO_2) coating will provide a suitable surface modified material for the phosphors because of their immiscibility with oxides and wide transparency range at a linear absorption coefficient level of $1\ cm^{-1}$ [27]. The phosphor particle surfaces are usually chemically unstable, the surface has many unsaturated bonds and some impurities can be easily absorbed, which will decrease the luminescence efficiency of the phosphors [28,29]. So, SiO_2 coating will appreciably improve the luminescence properties of the selected phosphors. With the recent demand in multimedia and high definition era for higher efficiency and better resolution in phosphors for displays and lighting, it is highly required to explore new phosphor materials or their additives.

Herein, $LnVO_4$: $Eu^{3+}_{0.05}$ (Ln = Gd, Y and Gd/Y), $Y_{0.95-x}VO_4$: Bi^{3+}_x, $Eu^{3+}_{0.05}$ ($0.001 \le x \le 0.02$ mol) and $Y_{0.949}VO_4$: $Bi^{3+}_{0.001}$, $Eu^{3+}_{0.05}$ @ SiO_2 sub micron sized powder phosphors have been synthesized by a modified colloidal precipitation technique, followed by heat treatment. Presently, the red emission from Eu^{3+} ions attributed to the hypersensitive $^5D_0 \rightarrow {}^7F_2$, transition at 616 nm has been improved significantly with fine tuning, mainly in three stages. Firstly, by fixing up the dopant Eu^{3+} concentration as 5 mol%, the effect of host composition with Gd and Y on fluorescence and pertinent optical properties have been investigated. Secondly, the luminescence intensity of the optimized phosphor $Y_{0.95}VO_4$: Eu^{3+} has been improved with the co-dopant, Bi^{3+} as a sensitizer. Finally, the luminescence intensity of the phosphor $Y_{0.949}VO_4$: $Bi^{3+}_{0.001}$, Eu^{3+} was further improved, remarkably by SiO_2 shell coating. Thus, the phosphor with composition $Y_{0.94}VO_4$: $Bi^{3+}_{0.001}$, $Eu^{3+}_{0.05}$ @ SiO_2 is optimized as a novel red emitting phosphor with enhanced luminescence intensity.

2. Experimental

2.1. Synthesis of $LnVO_4$: Eu^{3+} (Ln=Gd, Y and Gd/Y) and $Y_{0.95-x}VO_4$: Bi^{3+}_x, $Eu^{3+}_{0.05}$ ($0.001 \le x \le 0.02$ mol) powder phosphors

As we know that different preparation techniques may have some important effects on material microstructure, physical, optical and luminescence properties. Since, Levine and Palilla [30], first reported the modification of YVO_4 with Eu^{3+}, there after several methods have been developed to fabricate nano and microcrystalline YVO_4: Eu^{3+}, phosphors. Among those, a few are solid state reaction, hydrothermal synthesis, hydrolyzed colloidal reaction, sol–gel technique, induced precipitation and so on [12]. Among, these, colloidal precipitation is a promising route that can be well controlled through an appropriate choice of reaction parameters such as time, pH, chelating agent and surfactant. Here, the dopant Eu^{3+} concentration was fixed as 0.05 mol based on our previous reports [31].

Initially, yttrium oxide (Y_2O_3) (99.99%), gadolinium nitrate ($Gd(NO_3)_3 \cdot 06H_2O$) (99.99%), europium nitrate ($Eu(NO_3)_3 \cdot 05H_2O$) (99.99%), ammonium metavanadate (NH_4VO_3) of Aldrich make were dissolved in dilute nitric acid (HNO_3), under vigorous stirring and heating on a hot plate. After, complete dissolution a fixed volume of ethylene glycol was added as a surfactant and citric acid as a metal to metal chelating agent. The pH of the final solution was maintained at 9.0 with NH_4OH with drop wise addition. The resultant precipitate was allowed to stir for at least 3 h. Then the precipitate was ultrasonically treated for 30 min, followed by DI water wash, in order to remove the unreacted remnants. Ultrasonic treatment was adopted in order to obtain fine particle size moreover, to avoid the possible particle agglomerations. Ultrasonic treatment after colloidal precipitation can be treated as a ''modified'' colloidal precipitation technique. Further, the precipitate was dried in an electric oven at 120 °C. The dried powders were crushed in an agate mortar and then heat treated from room temperature to 1100 °C with 12 °C/min. as a heating rate and kept their for 3 h, in ambient atmosphere. The calcined samples were thoroughly washed with hot DI water and then dried at 120 °C for minimum 3 h. All the samples of the type $LnVO_4$: Eu^{3+} (Ln = Gd, Y and Gd/Y) were prepared in a similar fashion, according to their stoichiometric ratios. Besides, the phosphors with composition, $Y_{0.95-x}VO_4$: Bi^{3+}_x, $Eu^{3+}_{0.05}$ ($0.001 \le x \le 0.02$ mol) have been prepared as mentioned above. Additionally bismuth oxide (Bi_2O_3) (99.99%, Aldrich make) was incorporated with variable concentration as a sensitizer or co-dopant.

2.2. SiO_2 shell coating of the phosphor: $Y_{0.949}VO_4$: $Bi^{3+}_{0.001}$, $Eu^{3+}_{0.05}$

A variety of techniques are available for the core/shell type coating of SiO_2 which include inverse micelle method,

pretreatment steps in electro-less plating, double jet precipitation, layer by layer technique, template directed self-assembly and encapsulation of silica nanoparticles by in-situ polymerization [32–34], etc. Generally, these techniques need expensive and complicated equipment set-ups. However, in the present work silica shells on phosphor particles have been fabricated by hydrolysis of TEOS in an alcohol solvent in the presence of water and ammonia, which is a novel and inexpensive route. Initially, the optimized tetraethoxysilane (TEOS) ($C_8H_2OO_4Si$) (ACROS, USA) content with 2-propanol ($CH_3CHOHCH_3$) (J.T. Baker, USA) was stirred for a while for homogeneous mixing. The pH of the obtained solution was adjusted to 11.0 with ammonium hydroxide (NH_4OH). Then, ~3 g of $Y_{0.949}VO_4$: $Bi^{3+}_{0.001}$, $Eu^{3+}_{0.05}$ phosphor powder obtained in the above cited process was added to the TEOS solution. Then it was allowed to stir for 3 h with constant rpm for the homogeneous coating of Si-complex on the phosphor particles. The centrifuged mass was filtered and vacuum dried at 110 °C to remove the traces of solvent. The dried powders were further heat treated at 500 °C for 3 h, in an ambient atmosphere in a muffle furnace. Schematic diagram of the synthesis methodology for the fabrication of $Y_{0.949}VO_4$: $Bi^{3+}_{0.001}$, $Eu^{3+}_{0.05}$ @ SiO_2, core–shell structured phosphor is shown in Fig. 1.

2.3. Characterization

The crystalinity and phase purity of the synthesized powder phosphors have been investigated by Rigaku X-ray diffractometer D/max 2500 ultima having CuK_α radiation ($\lambda = 1.5406$ Å) at 40 kV tube voltage and 40 mA tube current. The XRD patterns measured with diffraction angle (2θ) ranging, $10^\circ \le 2\theta \le 70^\circ$. The PL spectra were measured with Scinco spectroflurometer with photomultiplier tube voltage 500, integration time 20 ms, excitation and emission slit as 5 nm. The chromaticity coordinates (x, y) as per Commission International de I'Clarage (CIE) were measured using Minolta Spectroradiometer. Before measuring, ~5 g of phosphor powder sample was spread onto a flat surface of 50 mm diameter and 1 mm thickness. The surface morphology and particle size of the synthesized phosphors were studied using Hitachi, S-4700 scanning electron microscope (SEM) with Horiba make EDAX attachment. The measurement conditions like accelerating voltage (kV), working distance (mm), magnification (× K) and scale bar employed for each sample were available on micrographs. Transmission electron microscopy (TEM) images of the phosphors were measured using JEOL-2000 EX, HR-TEM operated at 120 KV voltage.

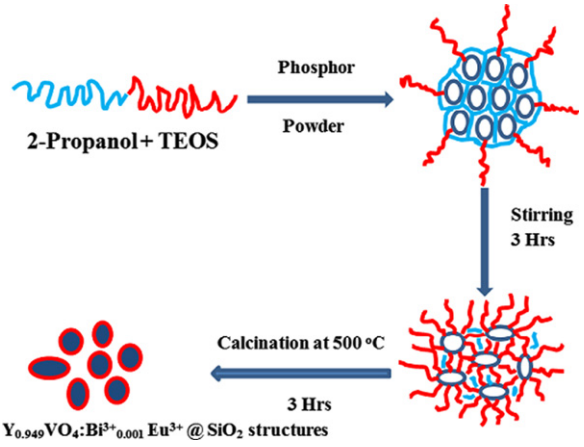

Fig. 1. Schematic diagram of the synthesis methodology for the fabrication of $Y_{0.949}VO_4$: $Bi^{3+}_{0.001}$, $Eu^{3+}_{0.05}$ @ SiO_2, core–shell structured phosphors.

3. Results and discussion

Fig. 2(a–f) shows the XRD patterns of solid solutions of the phosphors, $Y_{0.95-x}VO_4$: Bi^{3+}_x, $Eu^{3+}_{0.05}$ ($0.001 \le x \le 0.02$ mol). The $Y_{0.95}VO_4$: $Eu^{3+}_{0.05}$ phosphor has been co-doped with various concentrations of Bi^{3+}, ions. The exact chemical compositions of these phosphors is shown in Fig. 2. The observed diffraction peaks are indexed to (101), (200), (112), (220), (202), (301), (103), (321), (312), (400) and so on. These are noted to be well matched with the standard JCPDS file no: 170341 of YVO_4, which possess zircon type tetragonal structure. It can be seen from the XRD profiles, that the increased substitution of Y^{3+} to Bi^{3+} (from 0.001 to 0.02 moles) has not been shown any significant influence on the diffraction peak positions other than the intensities. The reason could be the doped Bi-concentrations were minimal. The diffraction peaks obtained for the sample with silica coating, i.e. $Y_{0.949}VO_4$: $Bi^{3+}_{0.001}$, $Eu^{3+}_{0.05}$ @ SiO_2 (Fig. 2(g)) have also been well matched with the JCPDS file no: 170341 of YVO_4, tetragonal phase. Silica coating has not shown any specific peaks corresponding to silica, which implies that the coating thickness might be in the range of a few nanometers. From the XRD data, it is revealed that there were no diffraction peaks corresponding to any impurity

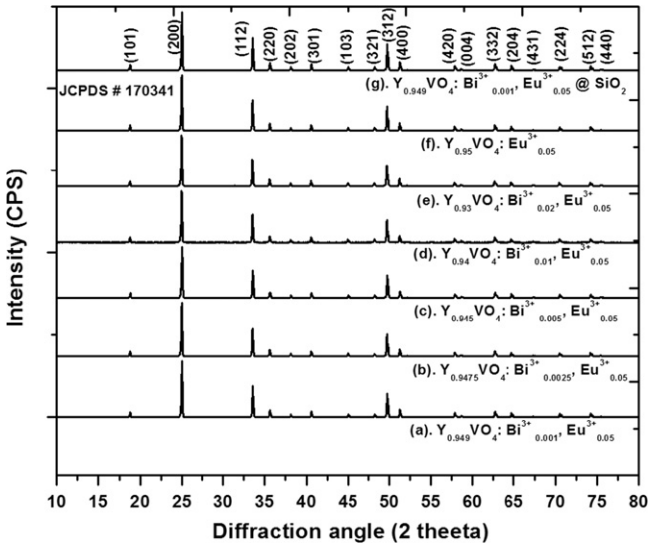

Fig. 2. XRD patterns of the phosphors: (a–f) $Y_{0.95-x}VO_4$: Bi^{3+}_x, $Eu^{3+}_{0.05}$ (where $x = 0$ –0.02 moles) and (g) $Y_{0.949}VO_4$: $Bi^{3+}_{0.001}$, $Eu^{3+}_{0.05}$ @ SiO_2.

or allotropic phases observed. This suggests that the crystalline and pure phase phosphor powders have been produced with the adopted synthesis technique. Since, the ionic radius of Eu^{3+} ($r=0.095$ nm) and Bi^{3+} ($r=0.096$ nm) are well close to that of Y^{3+} ($r=0.089$ nm), there will be more possible substitution for the Y^{3+}-sites with a little defect [6,35,36]. However, Neeraj et al. have reported that the structural studies of the system $Bi_xLn_{1-x}VO_4$: Eu^{3+} had shown the existence of two phases. Samples with $x \leq 0.65$ mol have shown tetragonal zircon phase, whereas for $x \geq 0.65$, the powder patterns indicated the mixture of both monoclinic fergusonite (due to $BiVO_4$) and tetragonal zircon phase (due to YVO_4). This could be due the fact that the ionic radius of Bi^{3+} ion is slightly larger than that of Y^{3+} ion; hence with the increased Bi^{3+} ions they were not able to substitute the Y^{3+} sites, successfully [4].

Fig. 3 shows the EDAX spectra of the phosphors: (a) $(Gd_{0.25,}\ Y_{0.75})_{0.95}VO_4$: $Eu^{3+}_{0.05}$, (b) $Y_{0.949}VO_4$: $Bi^{3+}_{0.001}$, $Eu^{3+}_{0.05}$, (c) $Y_{0.949}VO_4$: $Bi^{3+}_{0.001,}$ $Eu^{3+}_{0.05}$ @ SiO_2 and (d) $Y_{0.93}VO_4$: $Bi^{3+}_{0.02}$, $Eu^{3+}_{0.05}$. EDAX analysis elucidates the qualitative analysis of the elements of the respective phosphor composition, i.e. Gd, Y, O, V, Eu, Bi and Si. It is obvious from the spectra that no impurity elements were present due to a possible pick-up during co-precipitation reaction. The presence of elemental Si peak from Fig. 3(c) has evidenced the successful coating of SiO_2 shell on phosphor particles. The content of the elemental Si measured from EDAX technique is 1.98 wt% (2.79 atomic%) out of 4 vol% of TEOS solution used as a precursor. Furthermore, one can see clearly that the intensity levels of Bi peak increases (Fig. 3(b and d)), as the Bi-concentration increases from 0.001 to 0.02 mol. As per the Beer–Lamberts law, the peak intensities are proportional to the concentration of the respective element.

Fig. 4 shows the SEM images of (a) $Y_{0.95}VO_4$: $Eu^{3+}_{0.05}$, (b) $Y_{0.949}VO_4$: $Bi^{3+}_{0.001}$, $Eu^{3+}_{0.05}$, (c) $Y_{0.949}VO_4$: $Bi^{3+}_{0.001}$, $Eu^{3+}_{0.05}$ @ SiO_2 (10 K magnification) and (d) $Y_{0.949}VO_4$: $Bi^{3+}_{0.001}$, $Eu^{3+}_{0.05}$ @ SiO_2 (30 K magnification), powder phosphors. It can be seen from the micrographs, that the produced phosphor particles are loosely bound with size from 600 nm to 2 μm. Most of the particles roughly have a tetragonal like morphology [37]. The intense diffraction profiles obtained from the XRD measurements were supported by the prominent crystallites observed in SEM investigation. The smaller particles seems to be spread upon the bigger particles (Fig. 4(a, b)) are the crushed particles produced while hand grinding the lumps obtained from calcinations, using agate mortar and pestle [38]. Fig. 4(c and d) represents the SEM micrographs of the same composition phosphor, i.e. $Y_{0.949}VO_4$: $Bi^{3+}_{0.001}$, $Eu^{3+}_{0.05}$ @ $SiO_{2,}$ (c) 10 K magnification and (d) 30 K magnification. It is worth to focus attention on these two

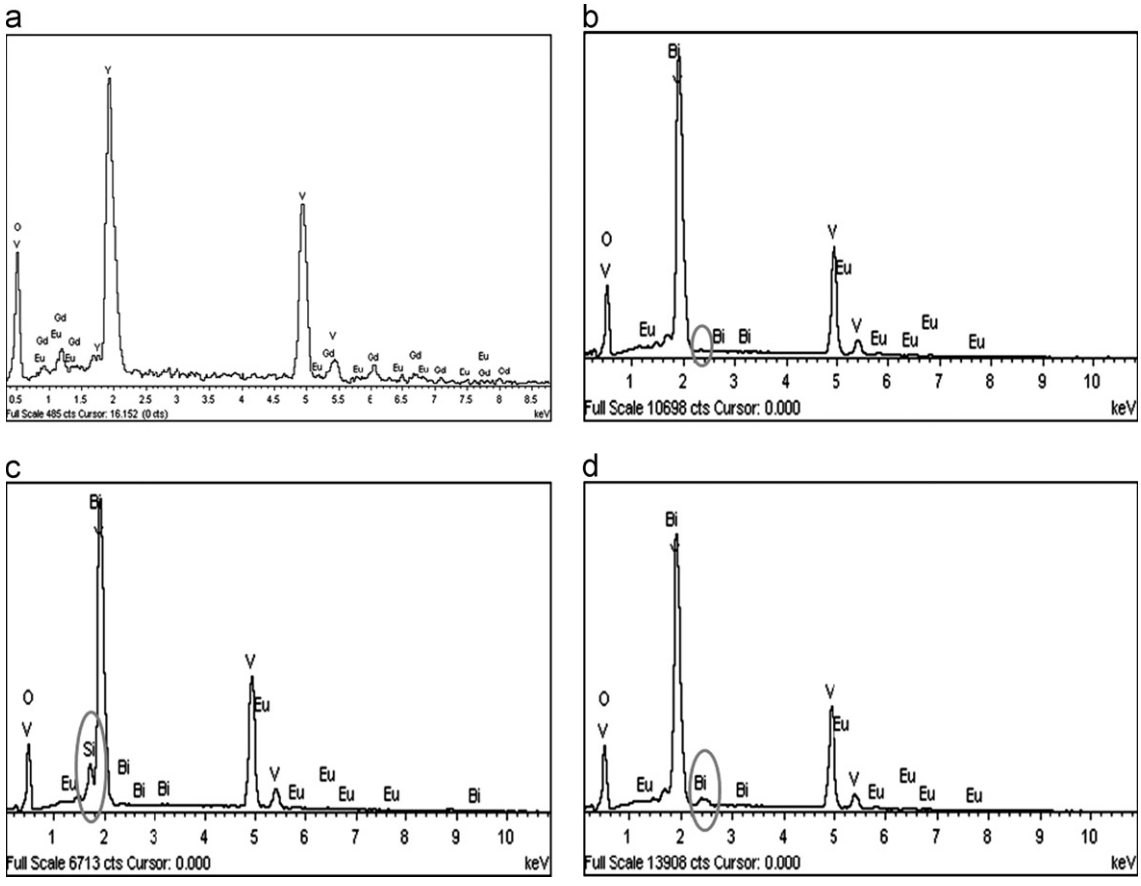

Fig. 3. EDAX spectra of the phosphors: (a) $(Y_{0.75},\ Gd_{0.25})_{0.95}VO_4$: $Eu^{3+}_{0.05}$, (b) $Y_{0.949}VO_4$: $Bi^{3+}_{0.001}$, $Eu^{3+}_{0.05}$, (c) $Y_{0.949}VO_4$: $Bi^{3+}_{0.001}$, $Eu^{3+}_{0.05}$ @ SiO_2 and (d) $Y_{0.93}VO_4$: $Bi^{3+}_{0.02}$, $Eu^{3+}_{0.05}$.

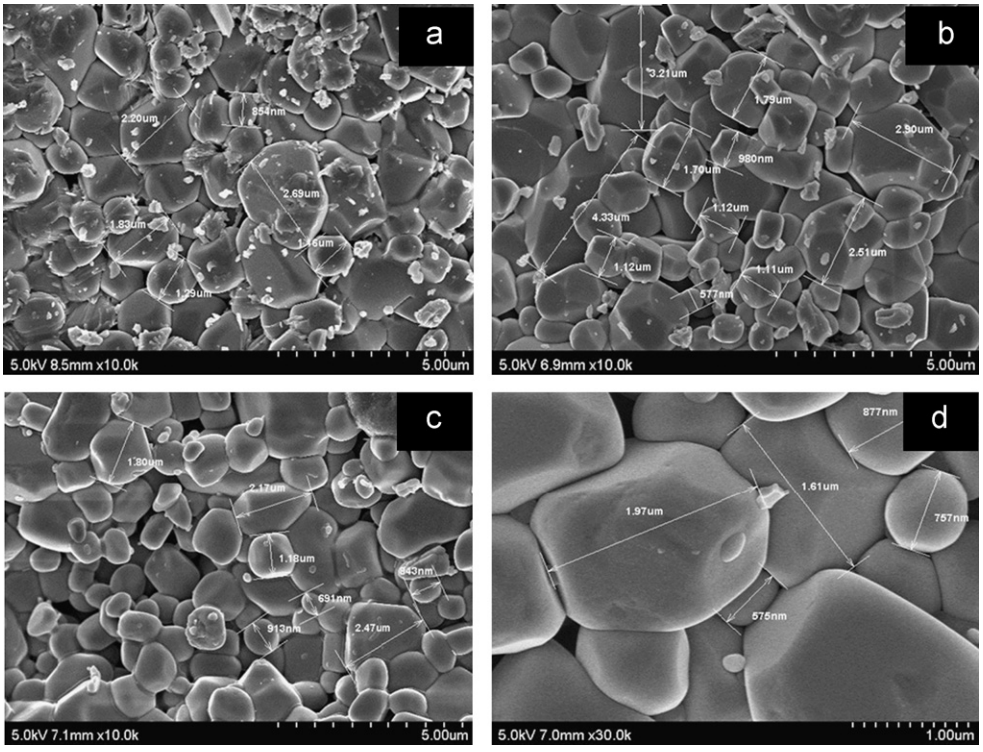

Fig. 4. SEM micrographs of the phosphors: (a) $Y_{0.95}VO_4$: $Eu^{3+}_{0.05}$, (b) $Y_{0.949}VO_4$: $Bi^{3+}_{0.001}$, $Eu^{3+}_{0.05}$, (c) $Y_{0.949}VO_4$: $Bi^{3+}_{0.001}$, $Eu^{3+}_{0.05}$ @ SiO_2 (10 K magnification) and (d) $Y_{0.949}VO_4$: $Bi^{3+}_{0.001}$, $Eu^{3+}_{0.05}$ @ SiO_2 (30 K magnification).

micrographs. One can see clearly that the surface of the phosphor particles (Fig. 4(d)) have improved significantly with clean and smooth surface owing to the SiO_2 shell coating. The improved modified surface morphology could contribute more in reducing the surface defects and light scattering effects in a greater way. The modified surface morphology as shown in Fig. 4(d) is an evidence for the successful coating of SiO_2 shell. Furthermore, silica coating on phosphor particles was also checked using transmission electron microscope (TEM). Fig. 5 shows the TEM image of the phosphor $Y_{0.949}VO_4$: $Bi^{3+}_{0.001}$, $Eu^{3+}_{0.05}$ @ SiO_2, which illustrates the transparent surface shell coating of SiO_2 on phosphor particles.

Fig. 6 shows the FT-IR spectra of (a) $Y_{0.95}VO_4$: $Eu^{3+}_{0.05}$, (b) $Y_{0.949}VO_4$: $Bi^{3+}_{0.001}$, $Eu^{3+}_{0.05}$ and (c) $Y_{0.94}VO_4$: $Bi^{3+}_{0.001}$, $Eu^{3+}_{0.05}$ @ SiO_2, phosphors. Modes in the region 400–2000 cm^{-1} observed are due to the V–O stretching vibrations of VO_4^{3-} and M–O (where M = Y, Bi and Eu) bonds. In the case of SiO_2 coated phosphor (Fig. 6(c)), besides the presence of the above characteristic absorption bands, absorption peaks at 1093 and 476 cm^{-1} are attributed to Si–O–Si asymmetrical stretching and Si–O bending vibration, respectively [39]. The weak signal due to M–O (where M = Y, Bi and Eu) bond is measured at around 449 cm^{-1}. The weak peak at 476 cm^{-1} (Fig. 6(c)) is attributed to Si–O bending mode. An intense and broad absorption peak in the wavenumber region 500–1000 cm^{-1} with its center at 836 cm^{-1} is attributed to V–O stretching mode. This suggests that the crystalline pure phase (YVO_4) has been

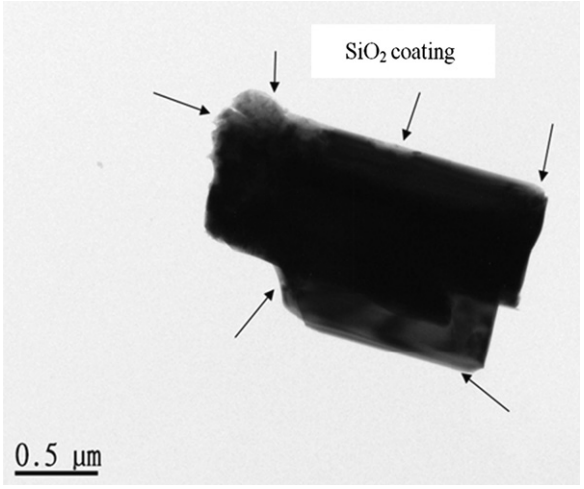

Fig. 5. TEM image of $Y_{0.949}VO_4$: $Bi^{3+}_{0.001}$, $Eu^{3+}_{0.05}$ @ SiO_2 powder phosphor.

formed for all the synthesized phosphors, agreeing well with the obtained results of XRD. It can be seen a prominent peak at 1093 cm^{-1} which is attributed to asymmetric stretching mode of Si–O–Si observed for SiO_2 coated sample, only (Fig. 6(c)). Generally, SiO_2 exhibits the absorption peaks due to Si–O–Si, asymmetric stretching at 1100 cm^{-1}, symmetric stretching at 803 cm^{-1}, Si–OH bond at 949 cm^{-1} and Si–O bending mode at 469 cm^{-1}, which may vary slightly with phosphor

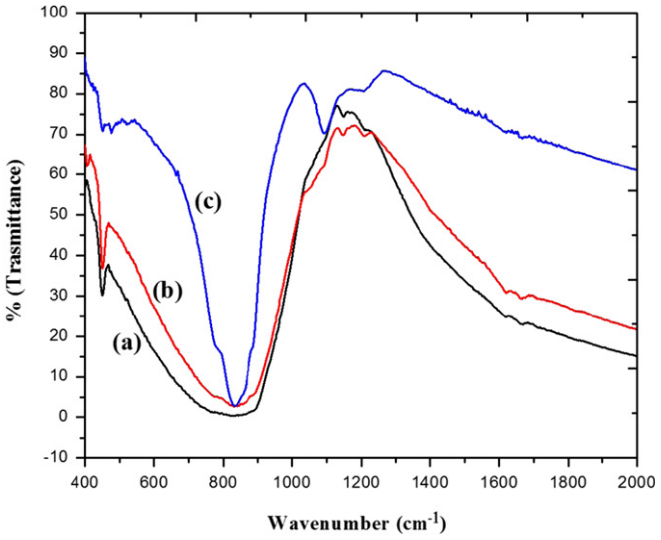

Fig. 6. FT-IR spectra of the phosphors: (a) $Y_{0.95}VO_4$: $Eu^{3+}_{0.05}$, (b) $Y_{0.949}VO_4$: $Bi^{3+}_{0.001}$, $Eu^{3+}_{0.05}$ and (c) $Y_{0.949}VO_4$: $Bi^{3+}_{0.001}$, $Eu^{3+}_{0.05}$ @ SiO_2.

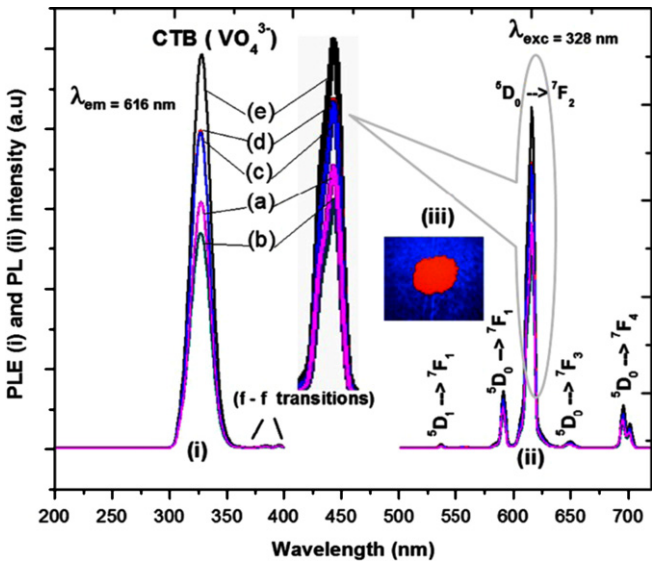

Fig. 7. Photoluminescence excitation (PLE) (i) and photoluminescence (PL) (ii) spectra of the phosphors, $Eu^{3+}_{0.05}$: (a) $Gd_{0.95}VO_4$, (b) $(Gd_{0.75},Y_{0.25})_{0.95}VO_4$, (c)$(Gd_{0.5},Y_{0.5})_{0.95}VO_4$, (d) $(Gd_{0.25}, Y_{0.75})_{0.95}VO_4$ and (e) $Y_{0.95}VO_4$. The inset (iii) shows the photograph, displays red emission from the phosphor, $Y_{0.95}VO_4$: $Eu^{3+}_{0.05}$ upon 365 nm near UV-excitation.

composition. The Si–OH group plays an important role in bonding silica on phosphor particles from the coating solution (TEOS) in forming YVO_4: Bi^{3+}, Eu^{3+} @ SiO_2 structures [34,40]. It can be seen from the spectra that the bands due to Si–O–Si symmetric stretching at 803 cm^{-1} and Si–OH band at 949 cm^{-1} were not clearly seen, the reason could be they might have overlapped with the broad band (500–1000 cm^{-1}) ascribed to V–O (VO_4^{3-}) [1,41].

Fig. 7 shows photoluminescence excitation (PLE) (i) and photoluminescence (PL) (ii) spectra of the phosphors, $Eu^{3+}_{0.05}$: (a) $Gd_{0.95}VO_4$, (b) $(Gd_{0.75},Y_{0.25})_{0.95}VO_4$, (c) $(Gd_{0.5},Y_{0.5})_{0.95}VO_4$, (d) $(Gd_{0.25}, Y_{0.75})_{0.95}VO_4$ and (e) $Y_{0.95}VO_4$, respectively. Excitation spectra were monitored by fixing the emission wavelength at $\lambda_{em}=616$ nm. A broad band can be seen from the excitation spectra in the near UV range, 300–357 nm with its center at 328 nm and several weak peaks in the range 350–400 nm. The broad band is attributed to the V^{5+}–O^{2-} metal-to-ligand charge transfer (CT) inside the $[VO_4]^{3-}$ ion, confirming that the emission occurs after the energy transfer from the excited vanadium to Eu^{3+}, ions [6,20,36]. According to the molecular orbital theory the broad band corresponds to the transition from the $^1A_2$ ($^1T_1$) ground state to $^1A_1$ (^1E) and ^1E ($^1T_2$) excited states of VO_4^{3-}, ions [39,42]. The weak absorption peaks in the longer wavelength region are originated from the general f–f transitions within the Eu^{3+}–$4f^6$ electronic configuration. These positions have not been changed with the host composition due to the shielding effect of 4f electrons by the outer shell 5s and 5p electrons [25]. The absorption intensity of the general f–f transitions of Eu^{3+}, ions in the longer wavelength region are very weak compared to VO_4^{3-} group. This indicates that the excitation of the Eu^{3+} ions are mainly through VO_4^{3-} groups, i.e. by the energy transfer from the VO_4^{3-} groups to Eu^{3+}, ions [43]. It can be seen from the intensity profile of VO_4^{3-}, CT absorption band with the substitution of Y to Gd sites, was initially decreased and then raised gradually with Y-concentration. Where, $Y_{0.95}VO_4$: $Eu^{3+}_{0.05}$ has shown a strong absorption among the others. Even though, the ionic radius of Eu^{3+} ($r=0.095$ nm) is relatively close to the ionic radii of the host rare earths, Y^{3+} ($r=0.089$ nm) and Gd^{3+} ($r=0.0938$ nm), the substitution of Eu^{3+} with Y^{3+} has shown better absorption properties. Fig. 8 shows the graphical representation of the relation between the CT band (CTB) intensity and yttrium concentration in moles.

The emission spectra as shown in Fig. 7(ii) (a–e), were monitored with the excitation wavelength, $\lambda_{exc}=328$ nm. The spectra consist of sharp peaks associated with the transitions from the excited $^5D_0$ level to the ground states of ^7F_j (where $j=1$, 2, 3 and 4) of Eu^{3+} dopant [25,42–44]. Of which, the major emissions are centered at 591 nm ($^5D_0 \rightarrow {}^7F_1$) magnetic dipole (MD) and at 616 nm ($^5D_0 \rightarrow {}^7F_2$) a hypersensitive electric dipole (ED) transition, were well corresponds to the orangish-red and red emission, respectively. Obviously, the emission spectra were noted to be dominated by the red $^5D_0 \rightarrow {}^7F_2$, hypersensitive transition due to the low local symmetry (D_{2d}, without inversion center) for the sites of Eu^{3+} in $LnVO_4$ (Ln = Gd, Y and Gd/Y) host lattices. The weak broad band at 649 nm is ascribed to $^5D_0 \rightarrow {}^7F_3$ and a doublet at 696, 701 nm is attributed to $^5D_0 \rightarrow {}^7F_4$, transition. The intensity distribution of $^5D_0 \rightarrow {}^7F_j$ transitions among the different j levels depends on the symmetry of the local environment around Eu^{3+}, ions and can be described by the Judd–Ofelt theory [45,46]. According to the selection rules, MD transition is permitted and ED transition is forbidden. In addition, a weak peak at 536.6 nm corresponds to

$^5D_1 \rightarrow {}^7F_1$ transition of Eu^{3+} from its high excited state of $^5D_1$ level, has also been observed. The presence of emission from the higher energy level is attributed to the low-energy vibration of VO_4^{3-} (836 cm^{-1}), groups. The multi-phonon relaxation by VO_4^{3-} was not able to bridge the gaps between the higher energy levels resulting in a weak emission from these levels [5]. Note that the $^5D_0 \rightarrow {}^7F_0$ transition of Eu^{3+} (which is only allowed for C_s, C_n, C_{nv} site symmetry) is absent from the emission spectra [34]. No emission from VO_4^{3-} group is observed with the excitation of 328 nm of UV, suggesting that the energy transfer from VO_4^{3-} to Eu^{3+} is quite efficient [5]. The intensity of hypersensitive transition $^5D_0 \rightarrow {}^7F_2$ with a fixed Eu^{3+} concentration (i.e. 5 mol%) was noted to be varied with the molar ratio of Gd to Y. The luminescence intensity trend observed has followed their respective CT excitation band intensities. The intensity of the red emission band ($^5D_0 \rightarrow {}^7F_2$) of $Gd_{0.95}VO_4:Eu^{3+}$ at 616 nm was initially reduced (for the composition, $(Gd_{0.75}, Y_{0.25})_{0.95}VO_4:Eu^{3+}_{0.05}$) and then increased gradually with increased yttrium concentration (from 0.5 to 0.95 mol) (Fig. 7(ii)). However, the composition, $Y_{0.95}VO_4:Eu^{3+}_{0.05}$ have exhibited a prominent emission profile as compared to the single or mixed host Gd/Y, vanadate phosphors. The intensity trend of the hypersensitive transition, $^5D_0 \rightarrow {}^7F_2$ with the variation in the host composition (Gd/Y) can be seen clearly in Fig. 7(i) (zoomed one). Moreover, Fig. 8 shows the graphical representation of the effect of Y-concentration on the intensity of hypersensitive transition, $^5D_0 \rightarrow {}^7F_2$. Fig. 7(iii) is the photograph which displayed red emission from the phosphor $Y_{0.95}VO_4:Eu^{3+}_{0.05}$, when exposed to 365 nm near UV-radiation.

In the present work initially, the effect of host composition, i.e. Gd, Y and Gd/Y on luminescence intensities were studied and found that $Y_{0.95}VO_4:Eu^{3+}_{0.05}$ is the better composition among the synthesized. In the second stage, we would like to see the sensitized luminescence effect of Bi^{3+} used as a co-dopant as $Y_{0.95-x}VO_4$: Bi^{3+}_x, $Eu^{3+}_{0.05}$ ($0.001 \leq x \leq 0.02$ mol). To increase the luminescence output and to avoid the concentration quenching, a small amount of co-activator (called as sensitizer) is desirable. The co-activator ion efficiently absorbs the excitation energy and then transfers it to the activator ions. Phosphors, which produce low luminescence intensity, can be explained normally by considering the poor intake of exciting radiation due to the pronounced reflectance losses coupled with non-radiative relaxation, at the surface states. The surface states, arising from discontinuity in lattice periodicity leads to numerous broken chemical bonds. To alleviate these problems, core/shell structured fabrication with SiO_2 has been practiced to stabilize the surface of phosphor particles. The process of luminescence quenching, could be suppressed if one were able to grow a shell of a material through which energy cannot be transferred. The idea of surface modification arose to improve the quantum efficiency by inhibiting energy transfer loss at the surface [47,48].

In view of the above merits in order to further improve the luminescence efficiency and color purity of the better phosphor composition, i.e. $Y_{0.949}VO_4$: $Bi^{3+}_{0.001}$, $Eu^{3+}_{0.05}$ as optimized in the second stage, a SiO_2 shell coating influence has also been investigated, as follows:

Fig. 9 shows the photoluminescence excitation (PLE) (i) and photoluminescence (PL) spectra (ii) of the phosphors with composition, (a–f). $Y_{0.95-x}VO_4$: Bi^{3+}_x, $Eu^{3+}_{0.05}$ ($0.001 \leq x \leq 0.02$) and (f) $Y_{0.949}VO_4:Bi^{3+}_{0.001}$, $Eu^{3+}_{0.05}$ @ SiO_2. It is obvious from Fig. 9, that the spectral profiles of the excitation and emission spectra observed for $LnVO_4$:

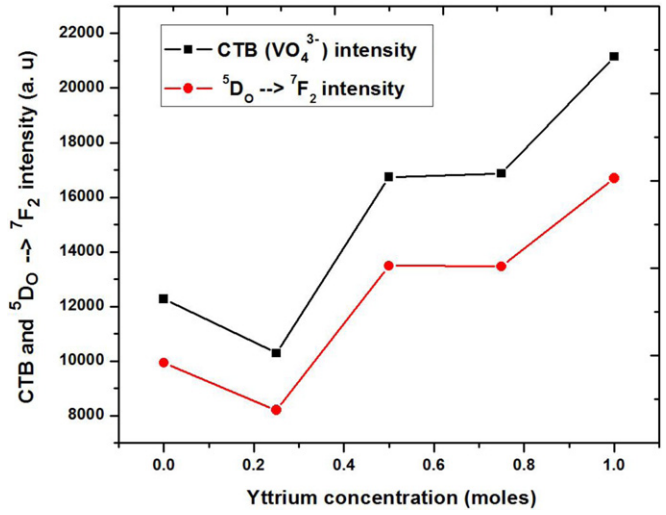

Fig. 8. Graphical representation of the effect of yttrium concentration on charge transfer band (CTB) and hypersensitive transition $^5D_0 \rightarrow {}^7F_2$, intensities.

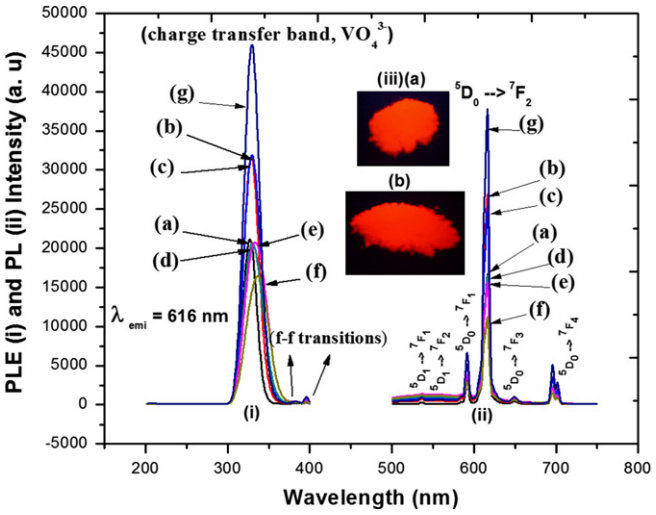

Fig. 9. Photoluminescence excitation (PLE) (i) and photoluminescence (PL) (ii) spectra of: (a) $Y_{0.95}VO_4:Eu^{3+}_{0.05}$, (b) $Y_{0.949}VO_4$: $Bi^{3+}_{0.001}$, $Eu^{3+}_{0.05}$, (c) $Y_{0.9475}VO_4:Bi^{3+}_{0.0025}$, $Eu^{3+}_{0.05}$ (d) $Y_{0.945}VO_4:Bi^{3+}_{0.005}$, $Eu^{3+}_{0.05}$, (e) $Y_{0.94}VO_4:Bi^{3+}_{0.01}$, $Eu^{3+}_{0.05}$, (f) $Y_{0.93}VO_4:Bi^{3+}_{0.02}$, $Eu^{3+}_{0.05}$ and (g) $Y_{0.949}VO_4:Bi^{3+}_{0.001}$, $Eu^{3+}_{0.05}$ @ SiO_2, phosphors. The insets (iii) are the photographs exhibiting red emission from the phosphors: (a) $Y_{0.949}VO_4$: $Bi^{3+}_{0.001}$, $Eu^{3+}_{0.05}$ and (b) $Y_{0.949}VO_4$: $Bi^{3+}_{0.001}$, $Eu^{3+}_{0.05}$ @ SiO_2 upon 365 nm near UV-radiation.

Eu^{3+} (Ln=Gd, Y and Gd/Y) were remained the same for $Y_{0.95-x}VO_4$: Bi^{3+}_x, $Eu^{3+}_{0.05}$, phosphors as well. It can be seen from the excitation and emission spectra (Fig. 9(i and ii)(b)) that the intensity of the CT band (VO_4^{3-}) and hypersensitive transition, $^5D_0 \rightarrow {}^7F_2$ of the phosphor $Y_{0.949}VO_4$: $Bi^{3+}_{0.001}$, $Eu^{3+}_{0.05}$ have improved 1.6 times, which was further enhanced 2.25 times significantly with SiO_2 coating (Fig. 9(i and ii)(g)) in comparison to $Y_{0.95}VO_4$: $Eu^{3+}_{0.05}$, phosphor (Fig. 10(i and ii)(a)). It is worth to note that as the Bi concentration increases the excitation band edges were found to be shifted to the longer wavelength side (Fig. 9(i)(a–f)). For e.g. the band edge of the excitation spectra moved from 326.88 nm (un-doped Bi)(Fig. 9(i)(a)) to 336.79 nm for the Bi concentration, 0.02 mol (Fig. 9(i)(f)). The red shift in the excitation band edge could be explained from the band structure calculation. It appears that the gap of yttrium vanadate mostly consists in a charge transfer between O_{2p} non-bonding levels of the valence band and V_{3d} levels of the conduction band [49,50]. When passing from yttrium to bismuth, the full O_{2p} levels shift to higher energy because of the interaction with the full Bi^2_{6S} levels, while the empty V_{3d} levels are shifted to lower energy through hybridization with the empty Bi_{6p} levels. Similar shifts have been reported with these solid solutions by various authors [6,14,51]. Quite interestingly, if we compare the phosphors, $Y_{0.949}VO_4$: $Bi^{3+}_{0.001}$, $Eu^{3+}_{0.05}$ without SiO_2 coating (Fig. 9(b)) and with SiO_2 coating (Fig. 9(g)), with silica coating the intensity of the CT band has increased, un-altering the absorption band edge. The reason could be the sensitizer Bi concentration was fixed as 0.001 mol in both of these phosphors. The strong luminescence observed for the phosphor $Y_{0.949}VO_4$: $Bi^{3+}_{0.001}$, $Eu^{3+}_{0.05}$ indicates that the energy transfer from VO_4^{3-} charge transfer state to Eu^{3+} ions via Bi^{3+}, sensitizer is more efficient for Bi, 0.001moles. The energy level diagram for VO_4^{3-} to Eu^{3+} energy transfer via Bi^{3+} ions and Eu^{3+} emission process has been shown as self-explanatory, Fig. 10 [6,20,52]. Furthermore, it is clearer

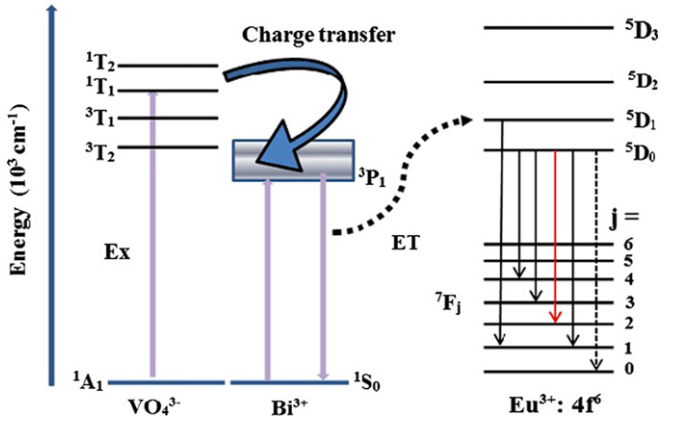

Fig. 10. Schematic diagram of VO_4^{3-}, Bi^{3+} and Eu^{3+} energy levels and the energy transfer process from $VO_4^{3-} \rightarrow Bi^{3+} \rightarrow Eu^{3+}$ in the system $Y_{0.95-x}VO_4$: Bi^{3+}_x,$Eu^{3+}_{0.05}$ ($0.001 \le x \le 0.02$ mol), where Ex, ET refers to excitation and energy transfer, respectively.

that beyond 0.001 mol. of Bi-content both the excitation and emission peak intensities have been diminished, due to the concentration quenching effect of Bi^{3+}, ions. Bi^{3+} will also bring new energy levels, probably associated with the contribution of the Bi_{6S} levels that can strongly modify the absorption but only favors the quenching of luminescence. These results indicate that the sensitization effect of Bi^{3+} ions on the Eu^{3+} emission varies with Bi^{3+}, concentration. For higher concentrations of Bi^{3+} ions (>0.001 mol), Bi^{3+} aggregates might be formed. These aggregates act as trapping centers and dissipate the absorbed energy non-radiatively, instead of transferring it to the Eu^{3+} activator ions [51]. The optimum Bi-concentration for better sensitized luminescence may depend on the host composition, particle size and dopant. Mahalley et al. have reported the optimum red emission with 0.2 mol% of Bi in $GdVO_4$ host [53]. Xu et al. have reported 1.5 mol% of Bi^{3+} as the optimized concentration for the efficient energy transfer for the system Gd_2O_3: Er^{3+}, Eu^{3+} [22]. The emission intensity of the phosphor $Y_{0.949}VO_4$: $Bi^{3+}_{0.001}$, $Eu^{3+}_{0.05}$ @ SiO_2 (Fig. 9(ii)(g)) was improved remarkably, compared to the phosphor without silica shell coating (Fig. 9(ii)(b)). This indicates that SiO_2 shells deposited on the phosphor particles have effectively reduced the surface defects. The modified particle surface resulted in the enhancement of luminescent intensity, by reducing the light scattering effects. This was supported by the SEM measurements, Fig. 4(d), where the phosphor particles surface morphology has become more clean and smooth with SiO_2 shell coating. Moreover, the presence of any defects in the crystal lattice of a phosphor material leads frequently to an alternative path ways for the excitation energy to be dissipated non-radiatively, instead of observing the luminescence [37]. Fig. 9(iii) insets show the photographs exhibiting red emission from the phosphors (a) $Y_{0.949}VO_4$: $Bi^{3+}_{0.001}$, $Eu^{3+}_{0.05}$ and (b) $Y_{0.949}VO_4$: $Bi^{3+}_{0.001}$, $Eu^{3+}_{0.05}$ @ SiO_2, upon 365 nm, near UV-irradiation. The photographs illustrate that the red emission from the phosphor $Y_{0.949}VO_4$: $Bi^{3+}_{0.001}$, Eu^{3+} @ SiO_2, Fig. 9(iii)(b) is the best among the synthesized phosphors.

Fig. 11 shows the graphical representation of the effect of Bi-concentration on hypersensitive transition, $^5D_0 \rightarrow {}^7F_2$ and CT band (VO_4^{3-}), intensity. The emission intensities of the transition, $^5D_0 \rightarrow {}^7F_2$, CT band intensity and the shift in the excitation band edge with Bi-concentrations have been summarized in Table 1. From the emission profiles of the produced phosphors (Figs. 7 and 9), it is obvious that the phosphor with composition, $Y_{0.949}VO_4$: $Bi^{3+}_{0.001}$, $Eu^{3+}_{0.05}$ @ SiO_2 has exhibited the improved luminescence intensity among the others.

The color purity of the synthesized phosphors would be gauged by evaluating the color coordinates (x, y), which have been computed based on their respective emission spectrum. Fig. 12 shows, the CIE 1931 chromaticity coordinates diagram. The color coordinates of the optimized phosphor $Y_{0.949}VO_4$: $Bi^{3+}_{0.001}$, $Eu^{3+}_{0.05}$ @ SiO_2 have been well fitted in the bright red region of the CIE,

Chromaticity diagram. In view of the above systematic investigations carried out, the luminescence intensity of $LnVO_4$: Eu^{3+} phosphors were improved significantly, by studying the effect of host composition (Gd, Y and Gd/Y), sensitized luminescence effect of Bi^{3+} as a co-dopant and finally, with silica shell coating as a protecting layer. Thus, the phosphor with composition $Y_{0.949}VO_4$: $Bi^{3+}_{0.001}$, $Eu^{3+}_{0.05}$ @ SiO_2 has been finely tuned for enhanced red emission for its suitable application in certain optical display devices or lighting.

4. Conclusions

In summary, it is concluded that the efficient $LnVO_4$: $Eu^{3+}_{0.05}$ (Ln=Gd, Y and Gd/Y), $Y_{0.95-x}VO_4$: Bi^{3+}_x, $Eu^{3+}_{0.05}$ ($0.001 \le x \le 0.02$) and $Y_{0.949}VO_4$: $Bi^{3+}_{0.001}$, $Eu^{3+}_{0.05}$ @ SiO_2 powder phosphors have been synthesized successfully, by a modified colloidal precipitation technique. XRD measurements revealed that the produced phosphors were well crystalline, phase pure and possess zircon type tetragonal structure. SEM micrographs illustrate that the synthesized phosphor particles are loosely bound with tetragonal like morphology with 600 nm to ~2 μm diameter grain size. SiO_2 coating on the selected phosphor particles have been characterized by SEM-EDAX, TEM, FT-IR and PL measurements. An intense broad charge transfer excitation band owing to VO_4^{3-} has dominated the f–f transitions of Eu^{3+} ions. This was found to be varied with host composition (Gd, Y and Gd/Y), Bi^{3+}-concentration and further improved significantly with SiO_2 coating. Moreover, the absorption band edges were noted to be shifted towards higher wavelength with Bi-concentration, owing to the presence of Bi–O bonds in addition to V–O. Emission peak intensities have been improved with the incorporation of Bi^{3+} ions, as a co-dopant. This is due to the efficient energy transfer from VO_4^{3-} group to the Eu^{3+} ions via Bi^{3+} ions with a metal to metal charge transfer from VO_4^{3-} to Bi^{3+}. It is worth to mention that the red

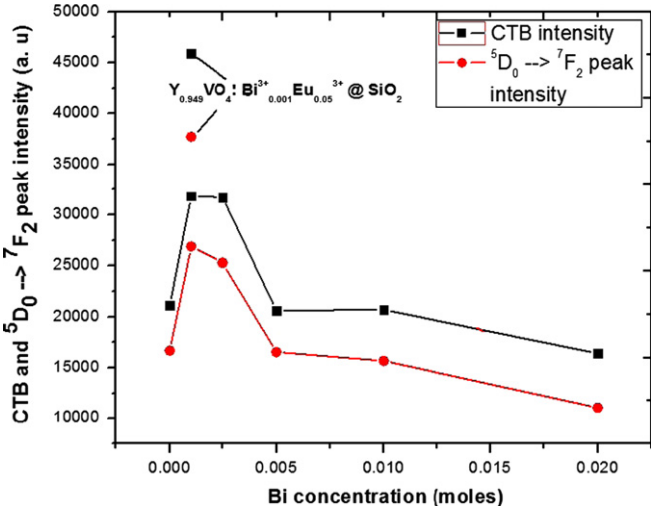

Fig. 11. Graphical representation displays the effect of Bi-concentration on charge transfer band (CTB) intensity and hypersensitive transition, $^5D_0 \rightarrow {}^7F_2$.

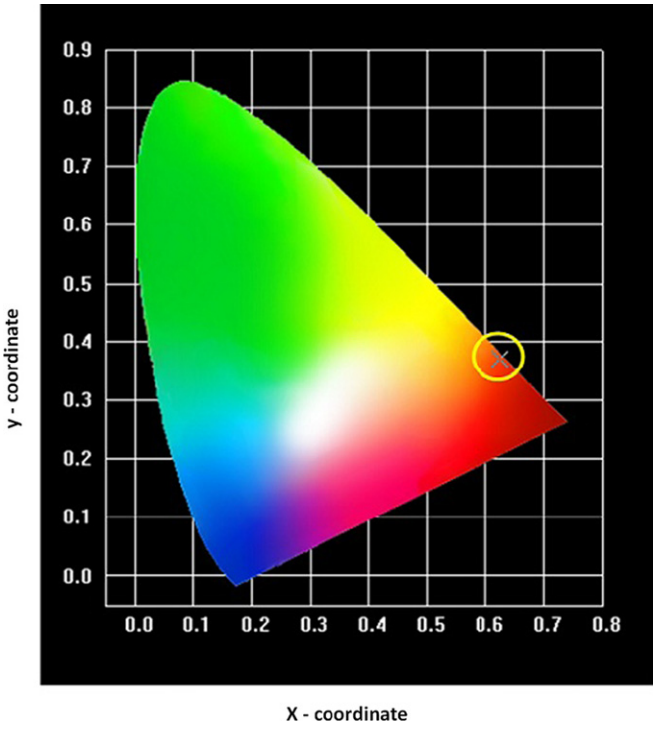

Fig.12. CIE, chromaticity diagram represents the placement of the color coordinates of $Y_{0.949}VO_4$: $Bi^{3+}_{0.001}$, $Eu^{3+}_{0.05}$ @ SiO_2, phosphor which was fitted in the bright red region. (For interpretation of the references to color in this figure legend, the reader is referred to the web version of this article.)

Table 1
PL intensity (a.u) of the hypersensitive transition ($^5D_0 \rightarrow {}^7F_2$) (at 616 nm), charge transfer band (CTB) intensity (a.u) and shift in the CTB edge of the synthesized powder phosphors.

Sl. no.	Phosphor	CT band intensity (a.u)	Shift in the CTB edge (nm)	Intensity of $^5D_0 \rightarrow {}^7F_2$ (a.u)
1	$Y_{0.95}VO_4$:$Eu^{3+}_{0.05}$	21,159	328.00	16,696
2	$Y_{0.949}VO_4$:$Bi^{3+}_{0.001}$, $Eu^{3+}_{0.05}$	31,713	329.10	26,877
3	$Y_{0.9475}VO_4$:$Bi^{3+}_{0.0025}$, $Eu^{3+}_{0.05}$	31,837	329.98	25,297
4	$Y_{0.945}VO_4$:$Bi^{3+}_{0.005}$, $Eu^{3+}_{0.05}$	20,710	329.98	16,556
5	$Y_{0.94}VO_4$:$Bi^{3+}_{0.01}$, $Eu^{3+}_{0.05}$	20,632	333.53	15,688
6	$Y_{0.93}VO_4$:$Bi^{3+}_{0.02}$, $Eu^{3+}_{0.05}$	16,417	336.79	11,086
7	$Y_{0.949}VO_4$:$Bi^{3+}_{0.001}$, $Eu^{3+}_{0.05}$ @ SiO_2	45,924	329.10	37,726

emission intensity owing to $^5D_0 \rightarrow {}^5D_2$ with $Y_{0.949}VO_4$: $Bi^{3+}_{0.001}$, $Eu^{3+}_{0.05}$ @ SiO_2 has enhanced 1.6 times than the phosphor $Y_{0.95}VO_4$: $Eu^{3+}_{0.05}$, which was further improved 2.25 times by SiO_2 shell coating. Finally, the phosphor with composition $Y_{0.949}VO_4$: $Bi^{3+}_{0.001}$, $Eu^{3+}_{0.05}$ @ SiO_2 has demonstrated an enhanced red emission due to $^5D_0 \rightarrow {}^5D_2$ transition at 616 nm and color purity ($x=0.6252$; $y=0.3707$). Thus, it could be suggested as a suitable red emitting phosphor for its suitable application in certain optical display devices or lighting.

Acknowledgments

One of the authors, URB would like to express his profound thanks to Dr. D.P. Amalnerkar, Executive Director and Dr. T.L. Prakash, Director of C-MET for their constant encouragement and cooperation towards this work.

References

[1] Z. Xia, D. Chen, M. Yang, T. Ying, Synthesis and luminescence properties of YVO_4: Eu^{3+}, Bi^{3+} phosphor with enhanced photoluminescence by Bi^{3+} doping, Journal of Physics and Chemistry of Solids 71 (2010) 175–180.

[2] S. Takeshita, T. Isobe, T. Sawayama, S. Niikura, Low temperature wet chemical precipitation of YVO_4: Bi^{3+}, Eu^{3+} nanophosphors via citrate precursors, Progress in Crystal Growth: Characterization of Materials 57 (2011) 127–136.

[3] M. Peng, L. Wondraczek, Orange to red emission from Bi^{2+} and alkaline earth co-doped strontium borate phosphors for white light emitting diodes, Journal of the American Ceramic Society 93 (5) (2010) 1437–1442.

[4] S. Neeraj, N. Kijima, A.K. Cheetham, Novel red phosphors for solid state lighting: the system $Bi_xLn_{1-x}VO_4$; Eu^{3+}/Sm^{3+} (Ln=Y, Gd), Solid State Communications 131 (2004) 65–69.

[5] K. Park, S.W. Nam, Red emitting $(Y_{0.5}Gd_{0.5})_{0.94-x}$ Al_xVO_4 ($0 \le x \le 0.04$) phosphors for plasma display panels applications, Optical Materials 32 (2010) 612–615.

[6] X.Y. Huang, J.X. Wang, D.C. Yu, S. Ye, Q.Y. Zhang, X.W. Sun, Spectral conversion for solar cell efficiency enhancement using YVO_4: Bi^{3+}, Ln^{3+} (Ln=Dy, Er, Ho, Eu, Sm and Yb) phosphors, Journal of Applied Physics 109 (2011) 113526-1–113526-7.

[7] X.Y. Huang, Q.Y. Zhang, Near infrared quantum cutting via cooperative energy transfer in Gd_2O_3: Bi^{3+}, Yb^{3+} phosphors, Journal of Applied Physics 107 (2010) 063505-1–063505-3.

[8] G.Q. Yao, J.H. Lin, I. Zhang, G.X. Lu, M.I. Gong, M.Z. Su, Luminescent properties of $BaMg_2Si_2O_7$: Eu^{2+}, Mn^{2+}, Journal of Materials Chemistry 8 (1998) 585–588.

[9] T. Hirai, T. Orikoshi, I. Komasawa, Preparation of Gd_2O_3:Eu^{3+} and Gd_2O_2S:Eu^{3+}phosphor fine particles using an emulsion liquid membrane system, Journal of Colloid and Interface Science 253 (2002) 62–69.

[10] W.J. Park, Y.H. Song, J.W. Moon, D.S. Jang, D.H. Yoon, Emission band change of $(Sr_{1-x}M_x)_3SiO_5$:Eu^{2+} (M=Ca, Ba) phosphor for white light sources using blue/near-ultraviolet LEDs, Journal of the Electrochemical Society 156 (2009) J148–J151.

[11] K. Rowotzki, M. Hasse, Colloidal YVO_4: Eu and $YP_{0.95}V_{0.05}O_4$: Eu nanoparticles: luminescence and energy transfer processes, Journal of Physical Chemistry B 102 (1998) 10129–10135.

[12] J. Wang, M. Hojamberdiev, Y. Xu, CTAB-assisted hydrothermal synthesis of YVO_4:Eu^{3+} powders in a wide pH range, Solid State Sciences 14 (2012) 191–196.

[13] J.H. Kang, W.B. Im, D.C. Lee, J.Y. Kim, D.Y. Jeon, Y.C. Kang, K.Y. Jung, Correlation of photoluminescence of (Y, Ln)VO_4: Eu^{3+} (Ln=Gd and La) phosphors with their crystal structures, Solid State Communications 133 (2005) 651–656.

[14] K. Hakouk, D. Giaume, P. Barboux, J. Sablayrolles, Solution synthesis of $Y_{1-x}Bi_xVO_4$ for optical applications, Journal of Luminescence 132 (2012) 1389–1393.

[15] Y. Wang, Y. Zuo, H. Gao, Luminescence properties of nanocrystalline YVO_4: Eu^{3+} under UV and VUV excitation, Materials Research Bulletin 41 (2006) 2147–2153.

[16] G. Blasse, A. Bril, Investigations on Bi^{3+}activated phosphors, Journal of Chemical Physics 48 (1968) 217–223.

[17] L. Chen, G. Yang, J. Liu, X. Shu, G. Zhang, Y. Jiang, Photoluminescence properties of Eu^{3+} and Bi^{3+} in YBO_3 host under vacuum ultraviolet/ultraviolet excitation, Journal of Applied Physics 105 (2009) 013513–013518.

[18] S. Takeshi, H. Ogato, T. Isobe, T. Wawayama, S. Niikura, Effects of citrate additive on transparency and photo stability properties of YVO_4:Bi^{3+}, Eu^{3+} Nanophosphor, Journal of the Electrochemical Society 157 (2010) J74–J80.

[19] L. Chen, K.J. Chen, S.F. Hu, R.S. Liu, Combinatorial chemistry approach to searching phosphors for white light-emitting diodes in (Gd–Y–Bi–Eu)VO_4 quaternary system, Journal of Materials Chemistry 21 (2011) 3677–3685.

[20] D. Chen, Y. Yu, P. Huang, H. Lin, Z. Shan, L. Zeng, A. Yang, Y. Wang, Color-tunable luminescence for Bi^{3+}/Ln^{3+}:YVO_4 (Ln=Eu, Sm, Dy, Ho) nanophosphors excitable by near-ultraviolet light, Physical Chemistry Chemical Physics 12 (2010) 7775–7778.

[21] G. Liu, Y. Zhang, J. Yin, W. Zhang, Enhanced photoluminescence of Sm^{3+}/Bi^{3+} co-doped Gd_2O_3 phosphors by combustion synthesis, Journal of Luminescence 128 (2008) 2008–2012.

[22] Q. Xu, B. Lin, Y. Mao, Photoluminescence of energy transfer between Er^{3+} and Bi^{3+} in Gd_2O_3: Er^{3+}, Bi^{3+}, Journal of Luminescence 128 (2008) 1965–1968.

[23] S. Takeshita, T. Isobe, T. Sawayama, S. Niikura, Effects of the homogeneous Bi^{3+} doping process on photoluminescence properties of YVO_4: Bi^{3+}, Eu^{3+} nanophosphor, Journal of Luminescence 129 (2009) 1067–1072.

[24] M. Bredol, U. Kynast, C.R. Ronda, Designing luminescent materials, Advanced Materials 7–8 (1991) 361–367.

[25] X. Xiao, G. Lu, S. Shen, D. Mao, Y. Guo, Y. Wang, Synthesis and luminescence properties of YVO_4:Eu^{3+} cobblestone like microcrystalline phosphors obtained from the mixed solvent–thermal method, Materials Science and Engineering B 176 (2011) 72–78.

[26] Y. Liang, R. Liu, W. Yan, X. Wu, Molten salt synthesis and photoluminescence of YVO_4: Eu microcrystalline phosphors, Advances in Materials Research 66 (2009) 65–68.

[27] C. Graf, D.L.J. Vossen, A. Imhof, A.V. Blaaderen, A general method to coat colloidal particles with silica, Langmuir 19 (2003) 6693–6700.

[28] Y.L. Shi, T. Asefa, Tailored core–shell–shell nanostructures: sandwiching gold nanoparticles between silica cores and tunable silica shells, Langmuir 23 (2007) 9455–9462.

[29] Y.X. Fu, Y.H. Sun, Comparative study of synthesis and characterization of mono-dispersed SiO_2 @ Y_2O_3: Eu^{3+} and SiO_2 @ Y_2O_3: Eu^{3+} @ SiO_2 core–shell structure phosphor particles, Journal of Alloys and Compounds 471 (2009) 190–196.

[30] A.K. Levine, F.C. Palilla, A new, highly efficient red-emitting cathodoluminescent phosphor (YVO_4: Eu) for color television, Applied Physics Letters 5 (1964) 118–121.

[31] U. Rambabu, D.P. Amalnerkar, B.B. Kale, S. Buddhudu, Fluorescence spectra of Eu^{3+}-doped $LnVO_4$ (Ln=La and Y) powder phosphors, Materials Research Bulletin 35 (6) (2000) 929–936.

[32] P. Schuetzand, F. Caruso, Electrostatically assembled fluorescent thin films of rare-earth-doped lanthanum phosphate nanoparticles, Chemistry of Materials 14 (2002) 4509–4516.

[33] S.R. Hall, S.A. Davis, S. Mann, Co-condensation of organo-silica hybrid shells on nanoparticle templates: a direct synthetic route to functionalized core–shell colloids, Langmuir 16 (2000) 1454–1456.

[34] G. Li, Z. Wang, M. Yu, Z. Quan, J. Lin, Fabrication and optical properties of core–shell structured spherical SiO_2 @ $GdVO_4$: Eu^{3+}

phosphors via sol–gel process, Journal of Solid State Chemistry 179 (2006) 2698–2706.
[35] H. Xu, C. Wu, H. Li, J. Chu, G. Sun, Y. Xu, Y. Yan, Synthesis, characterization and photocatalytic activities of rare earth-loaded $BiVO_4$ catalysts, Applied Surface Science 256 (2009) 597–602.
[36] L. Chen, K.J. Chen, C.C. Lin, C.I. Chu, S.-F. Hu, M.H. Lee, R.S. Liu, Combinatorial approach to the development of a single mass YVO_4: Bi^{3+}, Eu^{3+} phosphor with red and green dual colors for high color rendering white light-emitting diodes, Journal of Combinatorial Chemistry 12 (2010) 587–594.
[37] Y. Wang, W. Qin, J. Zhang, C. Cao, S. Lu, X. Ren, Photoluminescence of colloidal YVO_4: Eu/SiO_2 core/shell nanocrystals, Optical Materials 282 (2009) 1148–1153.
[38] H.D. Nguyen, S.I. Mho, I.H. Yeo, Preparation and characterization of nanosized (Y,Bi)VO_4:Eu^{3+} and Y (V,P)O_4:Eu^{3+} red phosphors, Journal of Luminescence 129 (2009) 1754–1758.
[39] Z. Hou, P. Yang, C. Li, L. Wang, H. Lian, Z. Quan, J. Lin, Preparation and luminescence properties of YVO_4: Ln and Y(V, P)O_4: Ln (Ln=Eu^{3+}, Sm^{3+}, Dy^{3+})nanofibers and microbelts by sol–gel/electro spinning process, Chemistry of Materials 20 (2008) 6686–6696.
[40] Y. Shang, P. Yang, W. Wang, Y. Wang, N. Niu, S. Gai, J. Lin, Sol–gel preparation and characterization of uniform core–shell structured $LaInO_3$:Sm^{3+}/Tb^{3+} @ SiO_2 phosphors, Journal of Alloys and Compounds 509 (2011) 837–844.
[41] H. Wang, M. Yu, C.K. Lin, J. Lin, Core shell structured SiO_2@YVO_4: Dy^{3+}/Sm^{3+} phosphor particles: sol–gel preparation and characterization, Journal of Colloid and Interface Science 300 (2006) 176–182.
[42] S. Choi, Y.M. Moon, K. Kim, H.K. Jung, S. Nahm, Luminescent properties of novel red-emitting phosphor: Eu^{3+}-activated $Ca_3Sr_3(VO_4)_4$, Journal of Luminescence 129 (2009) 988–990.
[43] G. Jia, Y. Song, M. Yang, K. Liu, Y. Zheng, H. You, Facile synthesis and luminescence properties of octahedral YVO_4: Eu^{3+} microcrystals, Journal of Crystal Growth 311 (2009) 4213–4218.
[44] B. Vengalrao, G. Bhaskar Kumar, M. Jayasimhadri, K. Jang, H.S. Lee, S.S. Yi, J.H. Jeong, Photoluminescence and structural properties of $Ca_3Y(VO_4)_3$: RE^{3+} (=Sm^{3+}, Ho^{3+} and Tm^{3+}) powder phosphors for tri-colors, Journal of Crystal Growth 326 (2011) 120–123.
[45] B.R. Judd, Optical absorption intensities of rare earth ions, Physical Review 127 (1962) 750–761.
[46] G.S. Ofelt, Intensities of crystal spectra of rareearth ions, Journal of Chemical Physics 37 (3) (1962) 511–520.
[47] J.K. Han, G.A. Hirata, J.B. Talbot, J. McKittrick, Luminescence enhancement of Y_2O_3: Eu^{3+} and Y_2SiO_5: Ce^{3+}, Tb^{3+} core particles with SiO_2 shells, Materials Science and Engineering B 176 (2011) 436–441.
[48] Y. Wang, X. Bai, T. Liu, B. Dong, L. Xu, Q. Liu, H. Song, Solvothermal synthesis and luminescence properties of mono disperse Gd_2O_3: Eu^{3+} and Gd_2O_3: Eu^{3+} @ SiO_2nanospheres, Journal of Solid State Chemistry 183 (2010) 2779–2785.
[49] M.R. Dolgos, A.M. Paraskos, M.W. Stoltzfus, S.C. Yarnell, P.M. Woodward, The electronic structures of vanadate salts: cation substitution as a tool for band gap manipulation, Journal of Solid State Chemistry 182 (2009) 1964–1971.
[50] W.J. Park, M.K. Jung, D.H. Yoon, Influence of Eu^{3+}; Bi^{3+} co-doping content on photoluminescence of YVO_4 red phosphor induced by UV excitation, Sensors and Actuators B 126 (2007) 324–327.
[51] M. Yu, J. Lin, Z. Wang, J. Fu, S. Wang, H.J. Zhang, Y.C. Han, Fabrication, patterning, and optical properties of nanocrystalline YVO_4: A (A=Eu^{3+}, Dy^{3+}, Sm^{3+}, Er^{3+}) phosphor films via sol–gel soft lithography, Chemistry of Materials 14 (2002) 2224–2231.
[52] M. Yu, J. Lin, J. Fang, Silica spheres coated with YVO_4:Eu^{3+} layers via sol–gel process: a simple method to obtain spherical core–shell phosphors, Chemistry of Materials 17 (2005) 1783–1791.
[53] B.N. Mahalley, S.J. Dhoble, R.B. Pode, G. Alexander, Photoluminescence in $GdVO_4$: Bi^{3+}, Eu^{3+} red phosphor, Applied Physics A 70 (2000) 39–45.